Optimization of Inductors Using Evolutionary Algorithms and Its Experimental Validation

Kota Watanabe[1], Felipe Campelo[1,2], Yosuke Iijima[3], Kenji Kawano[3], Tetsuji Matsuo[4], Takeshi Mifune[4], and Hajime Igarashi[1]

[1]Graduate School of Information and Technology, Hokkaido University, Sapporo 060-0814, Japan
[2]Departamento de Engenharia Elétrica, Universidade Federal de Minas Gerais, Belo Horizonte 31720-901, Brazil
[3]Taiyo Yuden Co., 5607-2 Nakamuroda-machi, Takasaki 370-3347, Japan
[4]Graduate School of Engineering, Kyoto University, Kyoto 615-8510, Japan

This paper presents parameter and topology optimization of inductor shapes using evolutionary algorithms. The goal of the optimization is to reduce the size of inductors satisfying the specifications on inductance values under weak and strong bias–current conditions. The inductance values are computed from the finite-element (FE) method taking magnetic saturation into account. The result of the parameter optimization, which leads to significant reduction in the volume, is realized for test, and the dependence of inductance on bias currents is experimentally measured, which is shown to agree well with the computed values. Moreover, novel methods are introduced for topology optimization to obtain inductor shapes with homogeneous ferrite cores suitable for mass production.

***Index Terms*—Finite-element (FE) method, immune algorithm, inductor, microgenetic algorithm, topology optimization.**

I. Introduction

INDUCTORS are important electric parts widely used in electric and electronic devices such as mobile phones and computers. Size reduction, operation at higher frequencies, and larger current tolerance in inductors have strongly been required from industries. While development of new materials having better characteristics is important to meet these requirements, improvements in inductor shapes are also indispensable. For the latter purpose, shape optimization based on evolutionary algorithms and computational electromagnetism is quite effective.

The goal of this study is to develop effective optimization methods for inductor shapes on the basis of computational electromagnetism. In the shape optimization, the size of the inductor is reduced as small as possible satisfying the specification on the inductance values under weak and strong current–bias conditions. Although evolutionary optimization based on computational electromagnetism has successfully been applied to various electric machines with magnetic materials, for example, motors, transformers, and magnets (e.g., [1] and [2]), there have been little numbers of reports on the shape optimization of inductors in spite of their importance.

In this work, the shape of inductors is optimized with parameter and topological approaches which have different merits. The parameter optimization, which determines prescribed design parameters at relatively low computational cost, is adopted to improve the shape of a typical inductor. It will be shown that the optimized shapes obtained by the immune algorithm (IA) and microgenetic algorithms ($\mu-$GA) [3], [4] are very similar and the resultant volumes are almost half of the original volume. Moreover, the measured inductance values of a trial inductor, produced on the basis of the optimization results, will be shown to agree well with computed values.

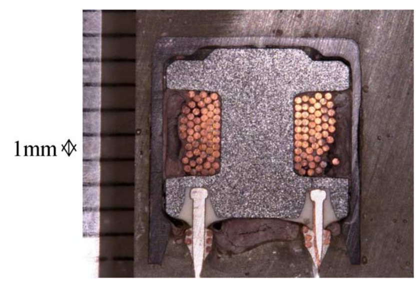

Fig. 1. Cross section of an inductor under consideration.

On the other hand, the topology optimization, which has more flexibilities than parameter optimization, is utilized to obtain novel inductor design. In this work, the shape of inductors is expressed with so called on–off method [5], which has widely been used for topology optimizations. However, there is a serious problem in this method; it often results in checkerboard-like shapes with many vacancies [6] for which high production cost are expected. To overcome this difficulty, shape regularization methods will be introduced. It will be shown that topology optimization with these approaches leads to homogenous inductor cores suitable for mass production.

II. Inductor Modeling

Fig. 1 depicts the cross section of an inductor which will be considered in this paper. This inductor, whose height and width are 6.9 $\times$ 7.5 mm (excluding sleeve), and inductance is 100 μH, consists of a bobbin-shaped ferrite core and a cupper coil surrounding it. In a typical application, this inductor is used for dc–dc converters, in which small ac currents with high dc bias current are applied to the inductor. Thus, the inductance property for dc bias current is important for this purpose.

The dc and ac B-H characteristics of the ferrite core are shown in Fig. 2(a) and (b). The former is measured by changing the dc

Manuscript received December 22, 2009; revised February 17, 2010; accepted February 26, 2010. Current version published July 21, 2010. Corresponding author: K. Watanabe (e-mail: watanabe@ssi.ist.hokudai.ac.jp).

Color versions of one or more of the figures in this paper are available online at http://ieeexplore.ieee.org.

Digital Object Identifier 10.1109/TMAG.2010.2044986

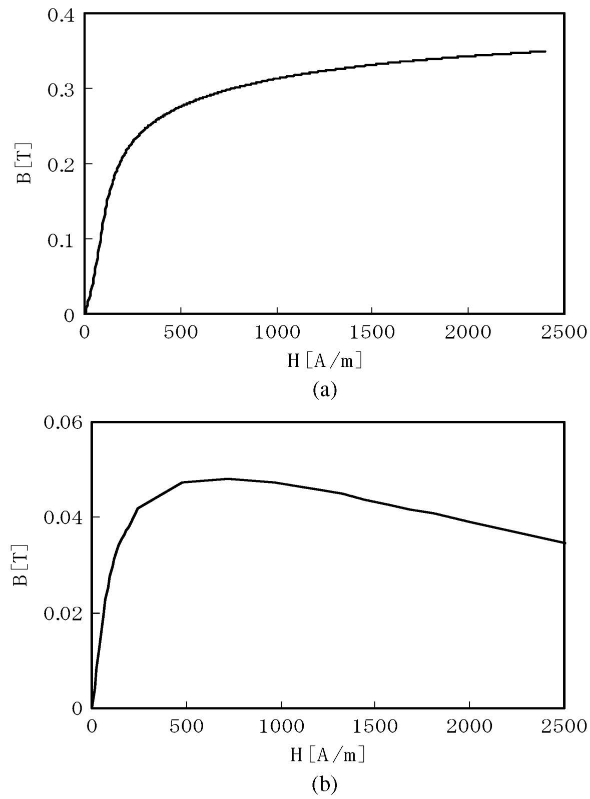

Fig. 2. B-H curves of ferrite core: (a) dc magnetic property; (b) ac magnetic property.

current bias, whereas the latter is measured for ac currents with small amplitude which are superimposed to the dc bias currents.

The inductance of the inductor is here characterized by two values: L_1 and L_2, defined at weak and strong current–bias conditions. Note that L_2 is expected to be smaller than L_1 because of magnetic saturation. In this paper, the bias currents are set to 0.2 and 1.0 (A), respectively. In the finite-element (FE) analysis of magnetic fields, operating points are determined by a dc field analysis based on the B-H curve shown in Fig. 2(a) and then small-signal analysis is performed with the curve in Fig. 2(b) where B/H represents the linearized permeability.

In this study, the 1/4 model shown in Fig. 3 is considered under the assumption of the up-down and left-right symmetries. The whole FE region, 40 $\times$ 40 mm, is discretized using the square elements for axially symmetric analysis. The numbers of FEs and unknowns are 62 500 and 63 001. The sleeve, lead-wires, and white resin shown in Fig. 1 are not modeled assuming that the magnetic effects from these parts are negligible. It will be shown that FE analysis under this assumption yields results which are in good agreement with the experimentally measured results.

III. Optimization Methods

In this paper, IA and $\mu-$GA are used for optimization. For completeness, they will be shortly described.

A. Immune Algorithm

The IA draws inspiration from the *clonal selection* principle, and combines local and global search characteristics. The procedures in IA are summarized below [3].

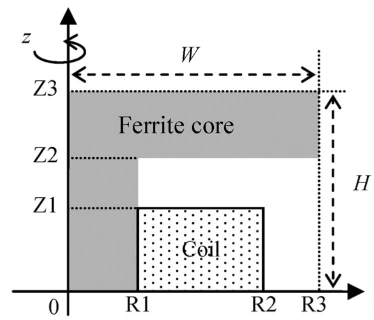

Fig. 3. Model for parameter optimization.

1) Generate an initial population of N random candidate solutions.
2) Evaluate the objective function and the constraint condition for each *antibody*.
3) Test a stop criterion. If it is satisfied, stop the procedures.
4) Eliminate P (in percent) low-ranking *antibodies*.
5) Generate *clones* for each surviving *antibodies*. The highest ranking *antibodies* receive a higher number of clones.
6) A small-amplitude Gaussian noise is applied to the *clones*, which are then evaluated over the objective and constraints. Only the best candidate solution from each subset of (parent *antibody plus clones*) is allowed to survive to the next generation.
7) Add randomly generated *antibodies* to replace the ones eliminated in Step 4, in order to keep the population size constant.
8) Back to step 2.

Steps 5 and 6 have a role of regulating the local search of the algorithm, while step 7 promotes global search. We can control the balance of local and global search by adjusting the parameters N and P.

B. Microgenetic Algorithm

On of the main differences between $\mu-$GA and the conventional GA is that very small populations are used in the former [4]. To avoid convergence to local optima, all individuals except the best ranking one are replaced by randomly generated individuals if the population is converged to a local optimum. In the following, there are procedures in $\mu-$GA.

1) Generate a small number N of initial individuals randomly.
2) Evaluate the objective function and the constraint condition for each individual, preserving the best one.
3) Test the stop criterion. If it is satisfied, stop the procedures.
4) Make pairs by randomly selecting two individuals, and the higher ranking individual for each pairs is called the parent.
5) Select two parents randomly, and apply the crossover operation to them to generate one or two children.
6) Compute the difference in the parameters between the best and the mean of the others. If the population falls into a local optimum, that is, the mean parameter difference becomes less than β (in percent), $N-1$ individuals are replaced by randomly generated ones. These individuals and the reserved best individual remain for the next generation.
7) Back to step 2 until the end criterion is satisfied.

TABLE I
PARAMETER OPTIMIZATION RESULTS

Methods	f	L_1 (μH)	L_2 (μH)	Volume ratio against the original model (%)
IA	2.71	100.03	80.11	55
μ-GA	2.74	99.99	82.54	56

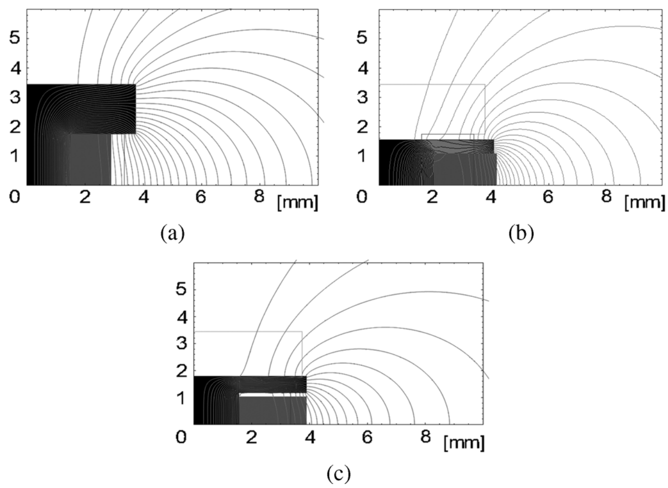

Fig. 4. Optimized shapes and flux distributions. (a) Original. (b) IA. (c) $\mu-$GA.

IV. Parameter Optimization

A. Optimization Setting

The parameter optimizations with five variables $(\mathrm{R1}, \mathrm{R3}, \mathrm{Z1}, \mathrm{Z2}, \mathrm{Z3})$ shown in Fig. 3 are performed using IA and $\mu-$GA. Note here that R2 depends on R1 and Z1 because the coil area is fixed to that of the original mass product model whose inductance in specification is 100 μH. The objective of this optimization is to reduce the inductor volume keeping the inductance to the following specifications: 1) $L_1 = 100$ μH, 2) $L_2 \geq 80$ μH. Considering these specifications in addition to requirement in reduction of the inductor volume, the objective function to be minimized is defined as

$$f = |L_1 \times 10^6 - 100| + 10^8 W^2 H + \text{penalty} \quad (1a)$$

$$\text{penalty} = \begin{cases} 80 - 10^6 L_2, & \text{if } L_2 < 80 \times 10^{-6} \\ 0, & \text{otherwise} \end{cases} \quad (1b)$$

where W and H [mm] denote the radius and the height of the inductor. Moreover, the geometrical constraint $\mathrm{Z1} \leq \mathrm{Z2} \leq \mathrm{Z3}$ is imposed. The parameters domains are set to $0 < \mathrm{R1} < 2$, $0.5 < \mathrm{R3} < 4$, $1 < \mathrm{Z1} < 4$, $1 < \mathrm{Z2} < 5$, $1 < \mathrm{Z3} < 5$ mms. The optimization parameters are set as follows: $N = 50$, $P = 50$ (in percent) and the maximum number of function evaluation is 5000 in IA, and $N = 5$, $\beta = 5$ and the maximum generation is 200 in $\mu-$GA.

B. Optimization Results

Table I summarizes the best solutions obtained by the IA and $\mu-$GA. We can see that the inductor volumes in the optimal solutions are around 55% of the original model shown in Fig. 1. Fig. 4 shows the cross section of the resultant inductors with magnetic flux lines. It can be seen that these optimal solutions have similar tendencies: low height $(\mathrm{Z3})$, wide width $(\mathrm{R3})$, and fat radius of core $(\mathrm{R1})$. It is suggested from the results that these features, being independent from optimization methods, are of importance for reduction in the volume with satisfaction of the constraints 1) and 2).

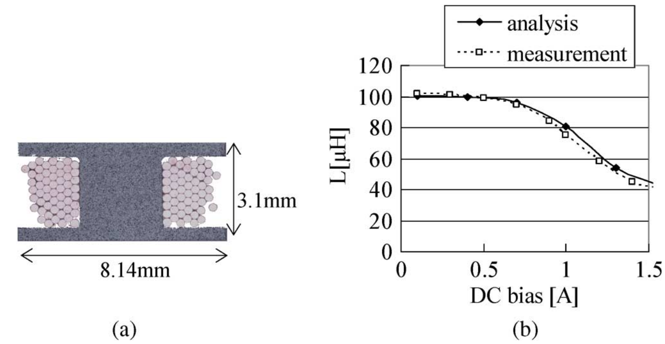

Fig. 5. Computed and experimentally measured results. (a) Trial piece produced based on IA result. (b) Inductance property against dc bias.

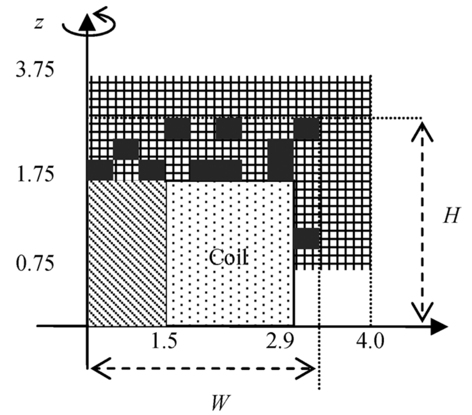

Fig. 6. Model for topology optimization Blobs represent cores in the optimization domain.

A trial inductor, whose cross-sectional view is shown in Fig. 5(a), is produced based on the solution obtained by IA to test reliability of numerical analysis. It can be seen in Fig. 5(b) that the computed dependence of the inductance on the bias current is in good agreement with the experimentally measured results. It is concluded that the present parameter optimization works well, which is shown to be effective for the volume reduction and have reliable results.

V. Topology Optimization

A. Optimization Setting

To increase the flexibility in the shape optimization, the topology optimization is applied to our problem. Fig. 6 shows the numerical model where the shape of the core is determined in the optimization domain represented by the grid lines, while the core shape in the center of the coil is unchanged. The core in the optimization domain is represented based on so-called on–off method [5] in which small rectangular cells are covered by the core material if their states are "on," but not otherwise. In this optimization, there are 20 $\times$ 15 cells, each of which is divided into four FEs.

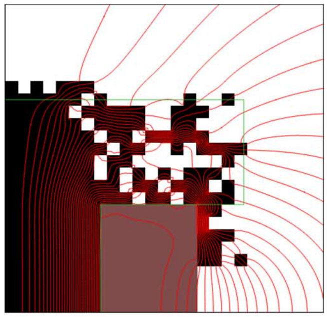

(a)

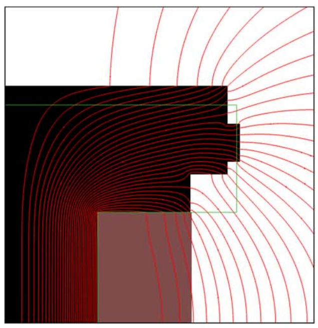

(b)

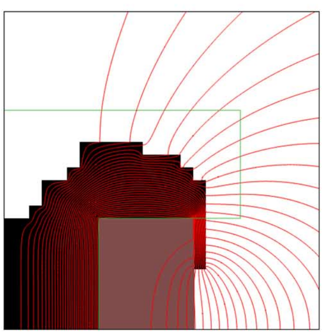

(c)

Fig. 7. Results of topology optimization. (a) Without regularization. (b) Method A. (c) Method B.

The objective function is defined by $f' = f + p'$, where f is given in (1a) and p' is the additional penalty term for regularization of topology optimization, which will be mentioned below. The IA is chosen for the optimization where the optimization setting is the same as that in the parameter optimization. The best solution in four trials for under each optimization condition will be shown below.

It is known that conventional topology optimization based on the on–off method often results in checkerboard-like shapes which would have high production costs [6]. To overcome this difficulty, two regularization methods are introduced. In method A, the total number of changes in the state of the cells, counted along r- and z-axes, is substituted into p'. The individuals in IA with checkerboard-like shapes are expected to have small possibilities for survival because their values of p' are relatively large. In method B, the penalty is defined by $p' = 10 \times N_{\rm on}/N_{\rm all}$, where $N_{\rm on}$, $N_{\rm all}$ denote number of cells whose states are "on," and total number of cells, respectively. The aim of this penalty is simultaneous reduction in the volume and complexity in the core shape. Note here that W^2H and p' are relevant to the overall and net volumes where the latter excludes the vacancies in the core.

TABLE II
TOPOLOGY OPTIMIZATION RESULTS

Regularization	f	L_1 (μH)	L_2 (μH)	W^2H (mm^2)	N_{on}/N_{all} (%)
Non	5.41	100.00	80.23	54.2	59.1
Method A	5.56	100.13	86.93	54.2	77.3
Method B	3.05	99.97	80.50	30.2	29.8

Fig. 7 shows the resultant shapes with magnetic flux lines. It can be seen that the optimization without regularization results in the checkerboard-like shape. In contrast, methods A and B yield homogenous cores, which would be more suitable for mass production in comparison with Fig. 7(a). Table II summarizes the properties of the optimal solutions. It can be seen that the values of L_1 are well close to the specified value and those of L_2 are greater than the lower limit mentioned in Section IV. From viewpoint of material cost, the shape obtained by method B, which has the minimum overall and net volumes, is superior over the others. The reason why the core resulted from method A is rather large would be that the penalty in this method tends to inhibit the change in the core shape in the evolutionary processes. The present regularization methods can be applied to other topology optimization problems.

VI. CONCLUSION

In this paper, parameter and topology optimizations for inductor shapes have been presented. It has been shown that the volume of the inductor can be significantly reduced by the parameter optimization keeping the specifications on the inductance values. The dependence of the computed inductance on the bias current agrees well with that experimentally measured. To avoid checkerboard-like shapes resulted from the topology optimization, new regularization methods have been introduced. As a result, they are shown to lead to homogenous ferrite cores which are expected to be suitable for mass production.

ACKNOWLEDGMENT

This work was supported in part by the JST "Seeds Innovation Program."

REFERENCES

[1] N. Bianchi and S. Bolognani, "Design optimisation of electric motors by genetic algorithms," *Inst. Electr. Eng. Proc.—Electr. Power Appl.*, vol. 145, no. 5, pp. 475–483, 1998.

[2] A. Canova, G. Gruosso, and M. Repetto, "Magnetic design optimization and objective function approximation," *IEEE Trans. Magn.*, vol. 39, no. 5, pp. 2154–2162, 2003.

[3] F. Campelo, F. G. Guimaraes, H. Igarashi, and J. A. Ramirez, "A clonal selection algorithm for optimization in electromagnetics," *IEEE Trans. Magn.*, vol. 41, no. 5, pp. 1736–1739, 2005.

[4] K. Krishnakumar, "Micro-genetic algorithm for stationary and non-stationary function optimization," in *Proc. SPIE 1196, Intell. Control Adapt. Syst.*, 1989, pp. 289–296.

[5] M. P. Bendsoe, "Optimal shape design as a material distribution problem," *Struct. Optim.*, vol. 1, pp. 193–202, 1989.

[6] O. Sigmund and J. Petersson, "Numerical instabilities in topology optimization, a survey on procedures dealing with checkerboards, mesh-dependencies and local minima," *Struct. Optim.*, vol. 16, pp. 68–75, 1998.